Experimental Investigation of Subsonic Combustion-Driven MHD Generator Performance

A. W. McClaine,* D. W. Swallom,† and R. Kessler‡
Avco Everett Research Laboratory, Inc., Everett, Massachusetts

Future mature combined-cycle MHD/steam electrical powerplants may use subsonic flow trains. To provide a data base of subsonic generator design and operating experience, an experimental program was begun in 1977 at the Avco Everett Research Laboratory. During this program, an MHD generator was operated with a subsonic flow train under both Faraday and diagonal loads. This paper reviews the work performed under this program and the results obtained.

Introduction

SYSTEMS analyses indicate[1] that the mature combined-cycle MHD/steam powerplant will be most efficient and cost effective when operated with a subsonic flow train. Before such flow trains can be built, experience must be gained in their design and construction. To contribute to the data base for the design and construction of subsonic flow trains, an experimental investigation was begun in 1977 at the Avco Everett Research Laboratory (AERL). The objectives of this program were: to operate an MHD generator at interaction-driven high subsonic flow velocities using ash-laden products of combustion as the working fluid, to test design concepts, to develop analytical design and predictive tools, and to identify specific problems associated with subsonic operation. This paper reviews the experimental work performed as part of this program.

Background

The first step in this program[2] involved testing an existing Mk VI generator that had been modified to promote subsonic operation in a 2.7 T peak magnetic field. The generator was operated at short circuit with a Faraday-loading arrangement and with an ash-injected oil combustor to simulate coal combustion. Subsonic operation was confirmed by a measurable rise in the combustor pressure with increasing interaction and by large increases in the static pressure measured at the generator entrance.

The second step, reviewed in this paper, was to investigate the performance characteristics of a subsonic generator operated at moderate load factors.[3-5] To perform this task a new copper-coil iron-core magnet capable of providing peak magnetic fields up to 4 T was used. In addition a new generator, designated the Reference Channel No. 3, was designed and built to operate at interaction-driven high subsonic velocities.

The work performed in this program extended the results presented by Ikeda et al.[6,7] by operating a subsonic generator at higher load factors and with ash-laden rather than ash-free flows.

Presented as Paper 84-0157 at the AIAA 22nd Aerospace Sciences Meeting, Reno, Nev., Jan. 9-12, 1984; received Feb. 14, 1984; revision received April 2, 1985. This paper is declared a work of the U.S. Government and therefore is in the public domain.

*Senior Scientist, Energy Technology Office.

†Principal Research Engineer, Energy Technology Office. Associate Fellow AIAA.

‡Vice President, Energy Technology Office. Associate Fellow AIAA.

The experimental work consisted of four sets of experiments as indicated in Table 1. The first two sets explored the performance characteristics of the Faraday-loaded generator at a particular load profile labeled the Faraday 1 load in Fig. 1. During the first set, the mass flow rate and the nitrogen-to-oxygen (N/O) ratio were varied widely around the design condition. During the second set, the flow conditions were varied over a more narrow range, but the generator was more thoroughly instrumented. In these tests, the sidewall interpeg voltages were measured at distributed locations and grouped at the entrance, middle, and exit regions of the generator. Because of the limited number of voltage transducers, the operating conditions were repeated for each grouping. Also, stagnation pressure profiles were taken across the diffuser from top wall to bottom wall and from sidewall to sidewall.

In the third set of experiments, the generator was loaded in a two-terminal diagonal mode. The generator was operated with bare and slag-covered walls to assess the effect of the cathode nonuniformities. As in the second set, the range of variation of the flow conditions was limited, but the flow conditions were repeated several times to measure interpeg voltages and diffuser stagnation pressure profiles. Finally, in the fourth set of experiments, the generator was reloaded in the Faraday mode but with a lower resistance (labeled Faraday 2 load in Fig. 1) to promote higher MHD interaction levels.

Generator Design and Diagnostics

The Mk VI test facility is of nominal 20 MW_{th} capacity with an ash-injected oil combustor to simulate coal combustion. The copper-coil iron-core magnet is capable of producing centerline peak magnetic fields of 4 T.

In Fig. 2, the two peg-type insulator walls of the reference channel 3 sandwich the two electrode walls. The electrode pitch is 18 mm and the channel length is 2500 mm. The channel is designed for constant velocity at the nominal operating condition and with a shallow divergence angle for the first 610 mm where the MHD interaction is low.

An interaction-driven subsonic generator operates with supersonic flow velocities at low magnetic field strengths. As the magnetic field is increased, the Lorentz force (i.e., MHD interaction), which opposes the flow direction, increases. This increasing force has the same effect on the flow as a reduction in the cross-sectional area. Thus, as the magnetic field increases, the supersonic flow velocities are reduced and the shock system, which normally resides in the diffuser of a supersonic generator, moves toward the nozzle. With a large enough interaction, the shock system is forced into the nozzle and will disappear altogether. Further increases in the interac-

tion cause increases in the combustor pressure. Since the entrance region of the generator is in a region where the magnetic field is low and thus the interaction is low, the entrance region of the subsonic generator must be lofted with a low-divergence angle to maintain high velocity.

Experimental data were collected using a digital data acquisition system that surveyed the diagnostics at 1 s intervals. Recorded data included reactant flow rates to the combustor, combustor stagnation pressure, static pressures in the generator and diffuser, flow rates and temperature changes of the cooling water to all flow train components, and the magnetic field strength. Electrode currents and interelectrode voltages were measured on both the anode and cathode walls. Interpeg voltages were measured at 10 peg row traverses that were distributed along the length of the generator for most of the tests and grouped at the entrance and exit of the generator for some of the tests. In addition, a stagnation pressure probe, located in the diffuser about 700 mm from the generator exit, was traversed across the flow from top wall to bottom wall and from sidewall to sidewall during many of the test conditions. Average axial conductivity was measured with the magnet off by placing a power supply from end to end of the generator and measuring the power supply current and the generator interelectrode voltages.

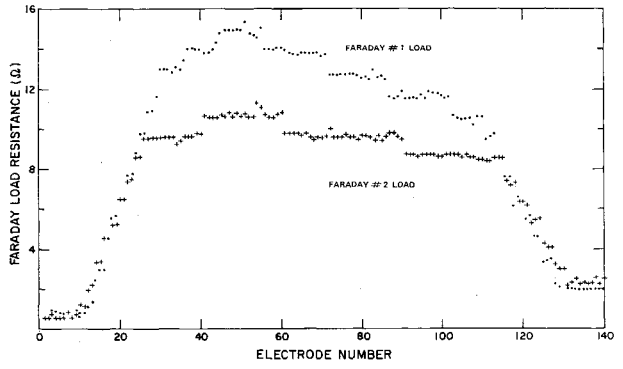

Fig. 1 Faraday load resistance profiles used in subsonic investigation.

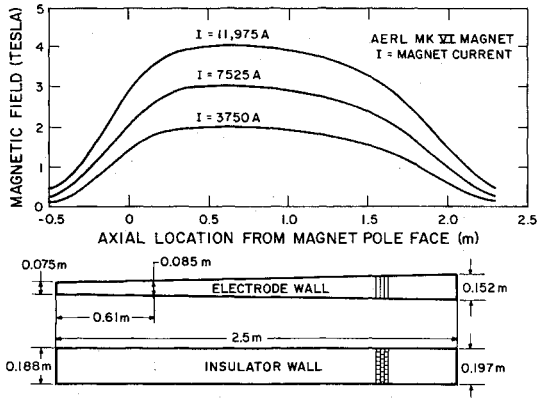

Fig. 2 Reference channel 3 dimensions and imposed magnetic field profiles.

Discussion

Combustor/Channel Interaction

When considering subsonic generators, a major concern is the possibility of interaction between the combustor and generator when the flow train is fully subsonic. MHD-generated pressure waves can propagate upstream into the combustor when the generator is operating in a subsonic flow regime. These waves could have a potentially harmful effect on the combustion processes.

During the testing, no effects due to the combustor/channel interaction were observed to be detrimental to generator performance. The generator performance appeared to be the same whether the flow train was fully subsonic or the nozzle was choked. A choked nozzle separates the combustor from the subsonic generator by a short supersonic region. Figures 3 and 4 display the static pressures, currents, and interanode

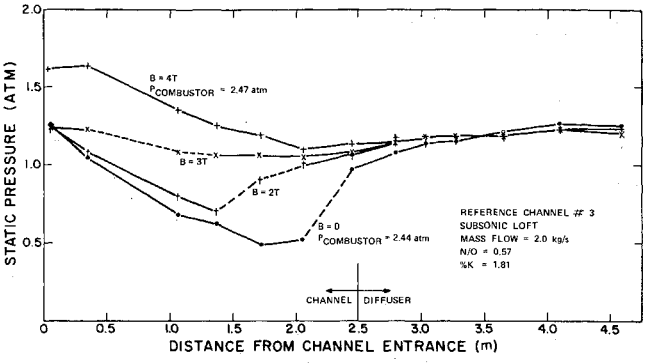

Fig. 3a Static pressure profiles at various interaction levels showing fully subsonic flow train at $B = 4$ T.

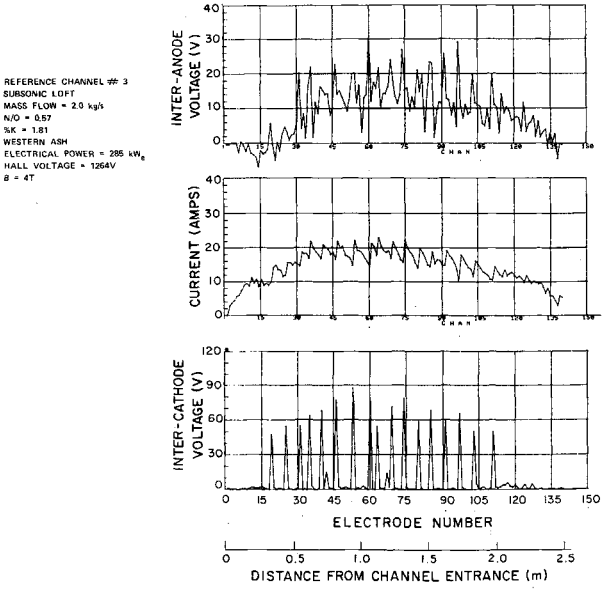

Fig. 3b Electrical profiles of fully subsonic flow train.

Table 1 Operating conditions explored during subsonic testing

Condition	Experiment set 1	2	3	4
Load	Faraday 1	Faraday 1	Diagonal	Faraday 2
Mass flow rate, kg/s	1.5–3.0	2.0–2.5	2.0–2.5	2.0–2.5
N/O, vol.	0.4–1.0	0.6–0.8	0.6–0.8	0.6–0.8
Peak magnetic field, T	0,2,3,4	0,2,3,4	0,2,3,4	0,2,4
Seed rate dry, wgt %	1.0	1.0	1.0	0.5–2.0
Ash (type)	Eastern	Eastern	Western	Western and eastern

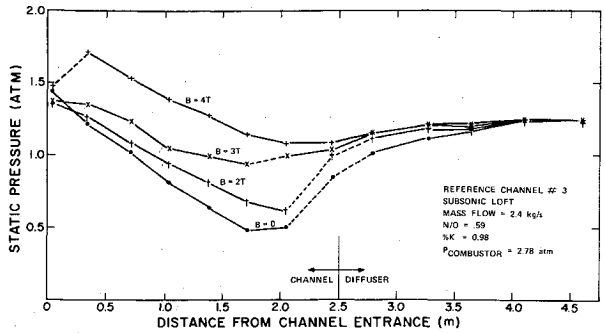

Fig. 4a Static pressure profiles at various interaction levels showing subsonic channel with choked nozzle.

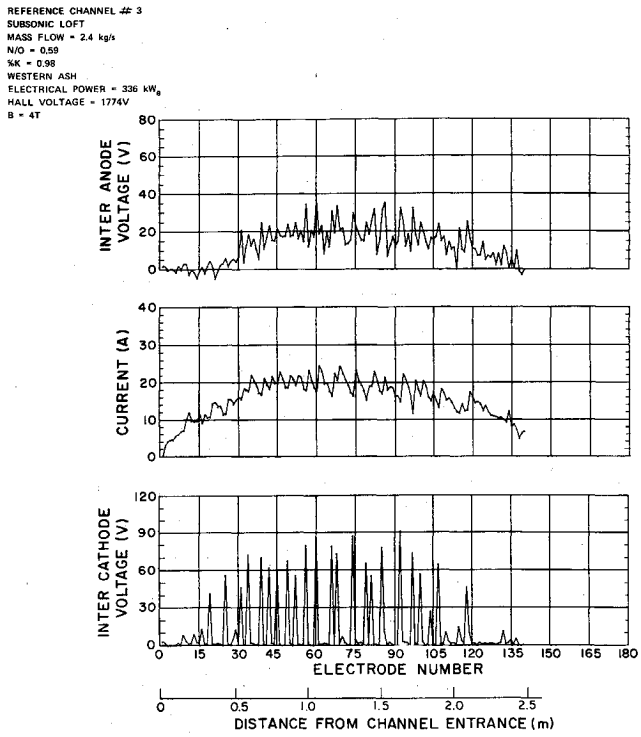

Fig. 4b Electrical distributions of subsonic channel with choked nozzle.

and intercathode voltages obtained for a fully subsonic flow condition and for a flow condition in which the nozzle was choked. Under the flow condition displayed in Fig. 3, the combustor pressure was observed to rise with the increase of the magnetic field. This pressure rise confirmed the fully subsonic nature of the flow train.

During the test program, the large combustor pressure increases predicted in pretest analyses were not observed. In only a very few conditions were combustor pressure rises observed at all. Under most conditions, a weak shock system at the entrance (indicated by the static pressure data) was observed. This may have been caused by small discontinuities between the nozzle and the channel.

The combustor pressure rise displayed in Fig. 3a, although only 0.5 psia, was positively observed as the magnetic field was adjusted up and down several times. Table 2 lists the reactant flow rates, power, Hall voltage, and combustor pressure for these conditions. The two conditions displayed differ by mass flow rate and seed concentration.

Perhaps the most significant result of this experiment is that the weak shock at the entrance of the generator caused no detrimental effect on generator performance. In larger, higher interaction machines in which MHD phenomena in the channel may affect combustion processes, subsonic generators may be lofted for a weak shock at the nozzle exit to separate the combustor from the generator.

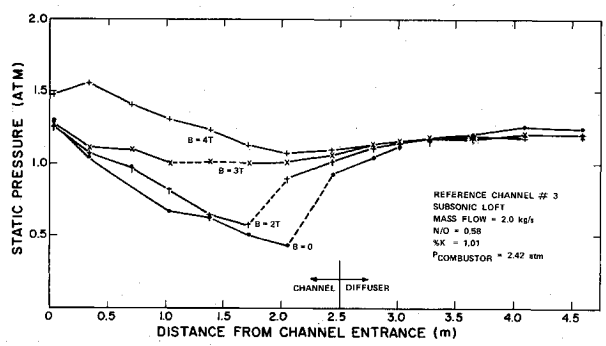

Fig. 5 Static pressure profiles showing movement of shock from channel exit to entrance.

Table 2 Experimental conditions for selected set 4 data

Total mass flow rate, kg/s	2.353	2.411	1.965	2.030	2.044
N/O, vol.	0.796	0.591	0.803	0.578	0.574
Seed rate, wgt %	0.996	0.978	0.954	1.009	1.808
Flow rates, kg/s					
No. 2 fuel oil	0.381	0.424	0.309	0.357	0.356
Oxygen (355 K)	0.881	1.065	0.735	0.906	0.901
Air (355 K)	1.047	0.878	0.884	0.728	0.717
K_2CO_3 (dry)	0.041	0.042	0.033	0.036	0.065
Ash (western)	0.002	0.002	0.004	0.002	0.004
Typical heat loss, kW_{th}					
Combustor	1005	1013	776	928	971
Nozzle	485	585	363	454	484
Channel, $B=0$ T	1737	1970	1371	1734	1664
$B=2$ T	1894	2101	1525	1839	1816
$B=4$ T	2117	2386	1741	2085	2095
Average conductivity at electrode 45, $B=0$ T, S/m	9.8	11.9	10.4	11.8	14.3
Selected data at 2 T					
Power, kW_e	110	161	91	126	166
Hall voltage, kV	0.971	0.943	0.966	0.785	0.768
Combustor pressure, atm	2.56	2.78	2.28	2.42	2.44
Selected data at 4 T					
Power, kW_e	278	336	195	243	285
Hall voltage, kV	1.945	1.774	1.748	1.547	1.264
Combustor pressure, atm	2.56	2.78	2.28	2.42	2.47

Generator Performance with Transonic Flow

Another area of investigation was the effects of mixed-flow operation on generator performance. An interaction driven subsonic generator operates with a fully supersonic or mixed (i.e., supersonic, shock, and subsonic) flowfield when the MHD interaction is not great enough to drive the flow fully subsonic. No noticeable detrimental effects from the shock system were observed in this set of experiments. This was probably due to the relatively weak nature of the shocks experienced in these experiments.

In some supersonic experiments, reductions in electrode current of up to 20% have been observed downstream of the shocks. This was not the case in the subsonic generator that operates close to Mach = 1 when supersonic. Figure 5 shows the movement of the shock upstream as the magnetic field is increased from 2 to 3 to 4 T as reflected in the static pressure profile. The movement of the shock is noted by the sharp rise in the static pressures in the 2 T and zero-field distributions. The shock at 3 T is not as visible. To determine that a shock resides in the channel at 3 T, the velocity at the first tap can be calculated by comparing the measured static pressure to the stagnation pressure at the first tap. Stagnation pressure at the first tap should be nearly the same as the combustor pressure because of the lack of any significant MHD interaction or friction between the combustor and first pressure tap. Using the standard isentropic relationship between stagnation pressure, static pressure, and the ratio of specific heats γ and assuming $\gamma = 1.15$, the Mach number at the first pressure tap for the data shown in Fig. 5 is 1.08 at magnetic fields of 0, 2, and 3 T and 0.94 at 4 T. The dashed lines indicate regions where shocks are thought to exist.

Figures 6-8 display the electrical characteristics at the magnetic fields of 2, 3, and 4 T, respectively. As the shock moves forward through the generator, no noticeable effects are observed on the electrical traces. Currents and interelectrode voltages increase because of the increased field. Table 2 displays the operating conditions for these data.

Diagonal Loading and Current Controls

Following the tests with the Faraday-loaded channel, a similar series of tests was performed with a diagonally loaded channel. Figures 9 and 10 compare power vs Hall voltage plots for both the Faraday- and diagonally loaded tests at mass flow rates of 2.0 kg/s and N/O ratios of 0.8.

Tables 3 and 4 display some of the reactant and thermal data for these figures. The peak diagonal power falls slightly below the corresponding Faraday data and the Hall voltages are nearly the same. The Faraday data were taken at a load factor on the short-circuit side of the optimum load factor point and thus the Faraday power is lower than it might be. In addition, the diagonal connection was complicated by the need for current controls to prevent current nonuniformities. As nondissipative current control circuits were not available for this test, 4 Ω resistors placed in the cathode/anode links were used as crude current controls. The effect of these current controls is shown in Fig. 10, where the power difference between the solid and the dashed lines represents the power dissipated in the link resistors.

The need for current controls in subsonic diagonally loaded generators is demonstrated by Fig. 11. This figure displays the electrical data collected with shorted diagonal connections. Electrode currents in excess of 45 A and interanode voltages

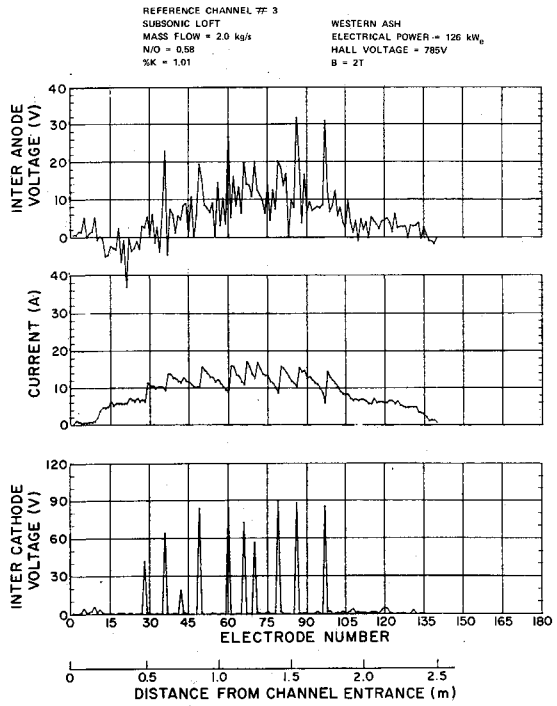

Fig. 6 Electrical profiles of generator with shock near the exit of the channel.

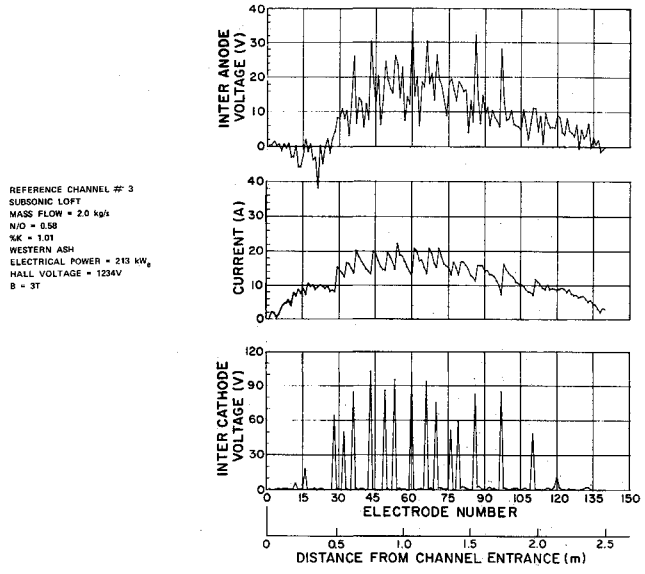

Fig. 7 Electrical profiles of generator with shock at midchannel.

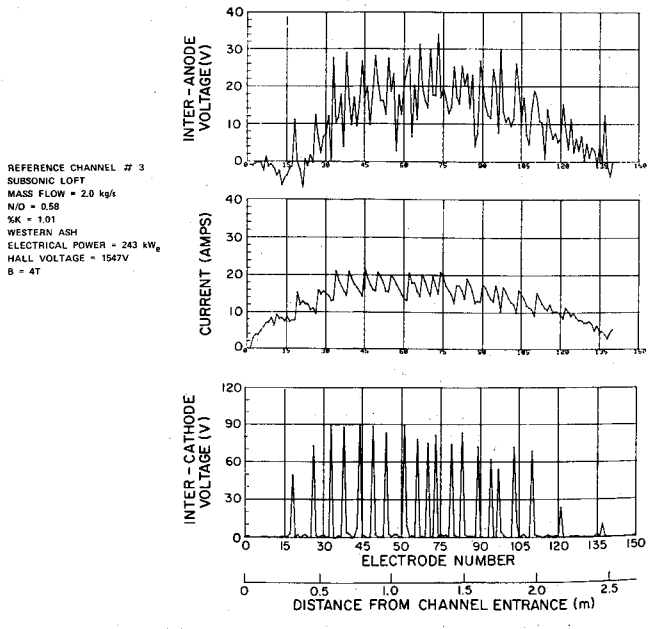

Fig. 8 Electrical profiles with flow train subsonic.

approaching 80 V were observed with the magnetic field strength at only 2 T. Nonuniformities such as these are similar to those observed previously in supersonic generators and can significantly shorten electrode life. This test was terminated because of these excessive currents and voltages. Figures 12 and 13 display the electrical data collected from the subsonic generator at the same flow conditions used in Fig. 11, both with 4 Ω resistors in the diagonal links. Even at 4 T (Fig. 13), the maximum currents are held below 24 A and the resulting

Table 3 Experimental conditions for selected set 2 data

Total mass flow rate, kg/s	2.494	2.515	1.985	2.036
N/O, vol.	0.779	0.584	0.777	0.599
Seed rate, wgt %	1.059	1.287	1.121	0.979
Flow rates, kg/s				
No. 2 fuel oil	0.400	0.443	0.328	0.369
Oxygen (355 K)	0.949	1.110	0.749	0.886
Air (355 K)	1.096	0.903	0.864	0.742
K_2CO_3 (dry)	0.047	0.057	0.039	0.035
Ash (eastern)	0.002	0.002	0.005	0.004
Typical heat loss, kW_{th}				
Combustor	776	772	654	658
Nozzle	281	343	216	333
Channel, $B=0$ T	1840	2084	1489	1732
$B=2$ T	1970	2250	1640	1810
$B=4$ T	2270	2618	1923	2158
Average conductivity at electrode 45, $B=0$ T, S/m	11.7	14.3	13.0	14.0
Selected data at 2 T				
Power, kW_e	186	235	166	185
Hall voltage, kV	0.934	0.904	0.955	0.891
Combustor pressure, atm	2.73	2.88	2.32	2.41
Selected data at 4 T				
Power, kW_e	438	526	319	359
Hall voltage, kV	2.036	1.742	1.643	1.589
Combustor pressure, atm	2.73	2.88	2.32	2.44

Table 4 Experimental data for a set 3 diagonal condition

Total mass flow rate, kg/s			2.07	
N/O, vol.			0.80	
Seed rate, wgt %			0.95	
Flow rates, kg/s				
No. 2 fuel oil			0.328	
Oxygen (355 K)			0.777	
Air (355 K)			0.928	
K_2CO_3 (dry)			0.035	
Ash (western)			0.004	
At $B=0$				
Average conductivity at electrode 45, s/m			10.0	
Channel heat loss, MW_{th}			1.42	
Combustor heat loss, MW_{th}			0.62	
Nozzle heat loss, MW_{th}			0.35	
Combustor pressure, atm			2.47	
Main load, Ω	7	10	18	43
At $B=2$ T				
Channel heat loss, MW_{th}	1.75	1.71	1.73	1.71
Power to main load, kW_e	77	92	89	63
Total power, kW_e	100	118	118	96
Hall voltage, kV	0.73	0.96	1.24	1.64
Main load current, A	107	96	72	38
At $B=3$ T				
Channel heat loss, MW_{th}	1.84	1.80	1.84	1.82
Power to main load , kW_e	157	170	173	123
Total power, kW_e	196	210	223	175
Hall voltage, kV	1.05	1.30	1.75	2.28
Main load current, A	151	131	99	54
At $B=4$ T				
Channel heat loss, MW_{th}	1.91	1.90	1.92	1.93
Power to main load, kW_e	230	229	223	161
Total power, kW_e	279	284	290	236
Hall voltage, kV	1.31	1.54	2.00	2.66
Main load current, A	176	149	112	62

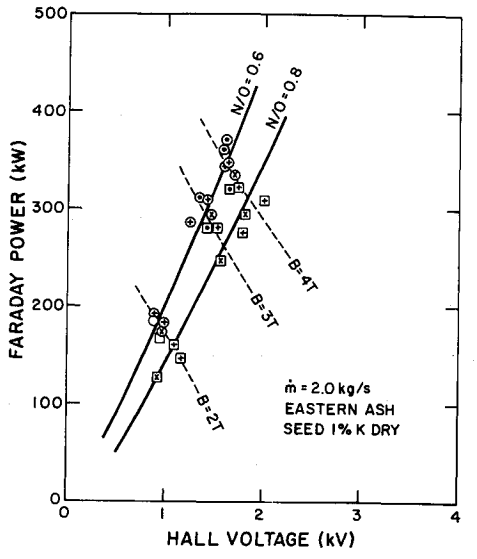

Fig. 9 Power vs Hall voltage plot of data from sets 1 and 2.

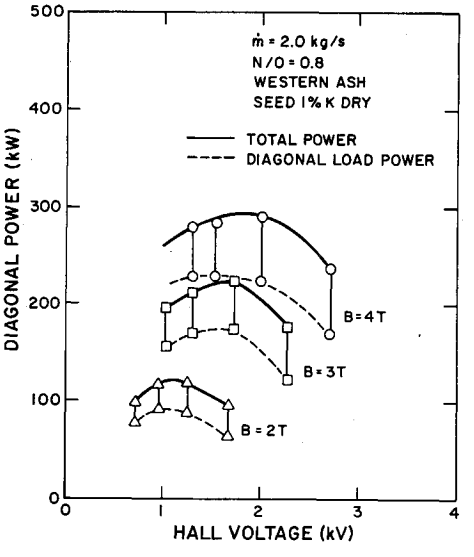

Fig. 10 Power vs Hall voltage plot of data from set 3.

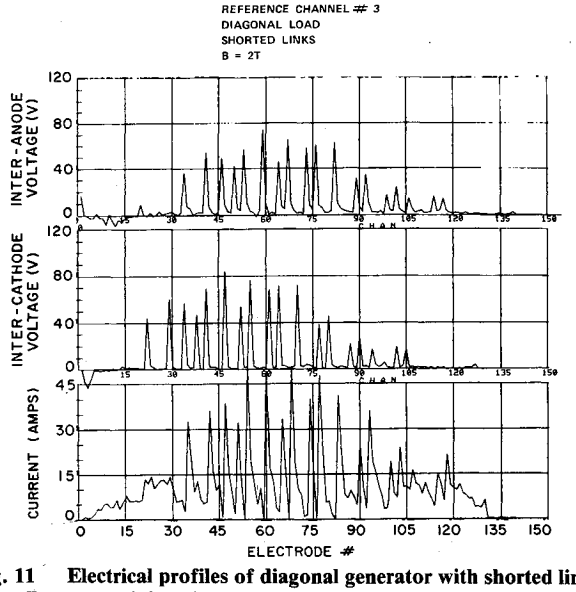

Fig. 11 Electrical profiles of diagonal generator with shorted links, mass flow rate = 2.0 kg/s, N/O = 0.6.

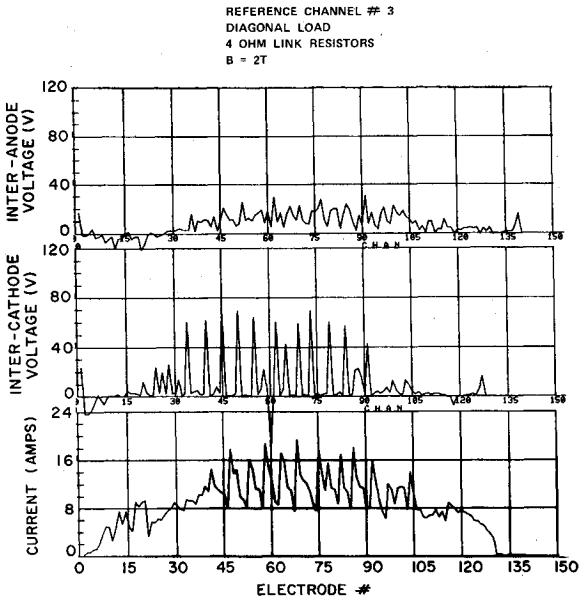

Fig. 12 Electrical profiles of diagonal generator with 4 Ω current control resistors in cathode/anode links, mass flow rate = 2.0 kg/s, N/O = 0.6.

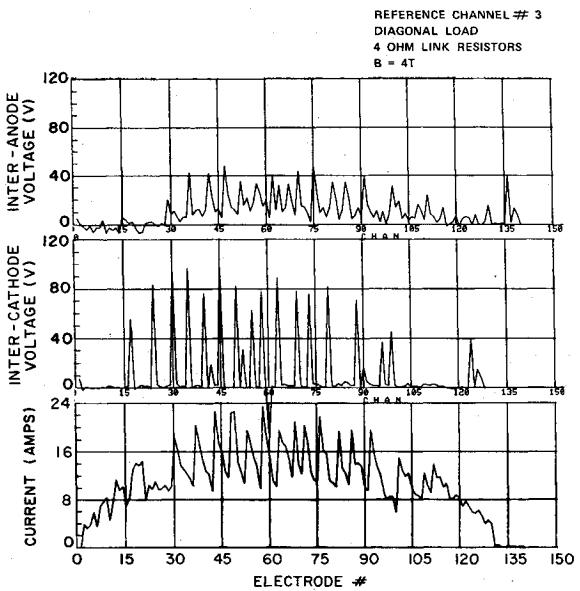

Fig. 13 Electrical profiles of diagonal generator with 4 Ω current control resistors in cathode/anode links, mass flow = 2.0 kg/s, N/O = 0.6.

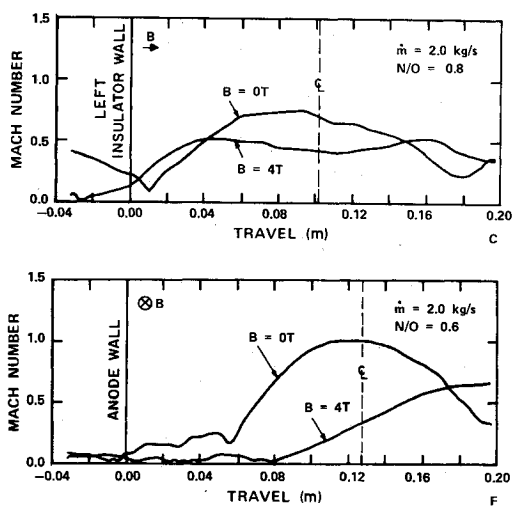

Fig. 14 Mach number profiles measured on subsonic generator.

interanode voltages are held below 40 V. These are both relatively safe levels.

Velocity Distribution Measurements

Velocity overshoots along the insulator walls of the channel and nonsymmetric velocity profiles between the electrode walls were measured with the stagnation pressure probe. Figure 14 displays typical profiles for subsonic operation and Fig. 15 typical profiles for supersonic operation. In both figures, the sidewall velocity overshoot is evident. Also, in both figures one can see a nonsymmetric velocity profile that confirms the existence of the three-dimensional effects described in Refs. 8 and 9. In Fig. 15a, the magnetic field direction was reversed from normal to verify that the peak velocity moves from the centerline toward the cathode as the magnetic field is increased. (The cathode is defined here as the electrode emitting electrons to the plasma.)

The nonsymmetry evident close to the walls is probably caused by the probe affecting the flowfield at its cross plane.

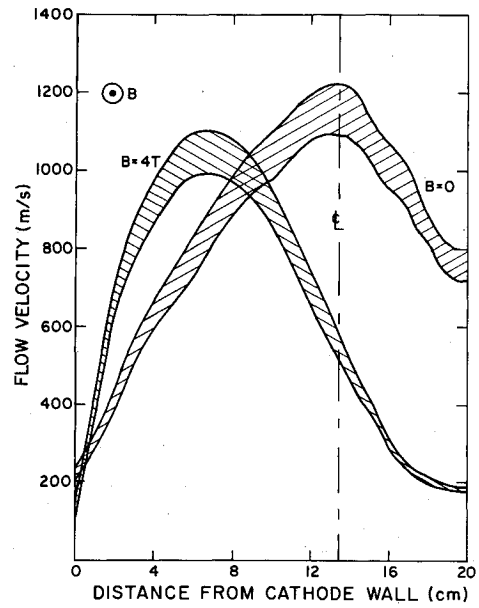

Fig. 15a Velocity profiles measured on supersonic generator from top wall to bottom wall.

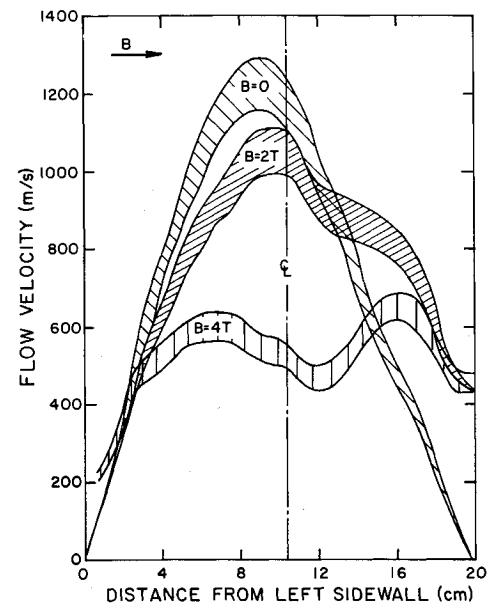

Fig. 15b Velocity profiles measured on supersonic generator between side walls.

Conclusions

In conclusion, subsonic generator operation was found to be no more difficult than supersonic generator operation. Reference Channel No. 3 has been operated for more than 75 thermal cycles with a total of 172 thermal and 52 power hours. Electrode lifetime under subsonic operation appears to be no different than the lifetime under supersonic operation. Problems associated with combustor/generator interactions and problems under operation with a shock in the generating section were not observed. Operation of the subsonic generator with a diagonal load was found to exhibit the same types of current nonuniformity problems as had been observed in supersonic generators.

Finally, during this program, a stagnation pressure probe that allows the measurement of stagnation pressures across the flow in the hot slag-laden gases of the diffuser was developed. The probe measurements verified the existence of velocity overshoots on the sidewalls and nonsymmetric velocity profiles between the two electrode walls.

Acknowledgments

This work was supported by the U.S. Department of Energy under Contract DE-AC22-80ET15614.

References

[1]Hals, F. A., Pian, C. C. P., Demirjian, A. M., Sadovnik, I., and Stankevics, J. O., "Results from Comparative Analysis of Different MHD Generator and Power Train Designs for Early Commercial Power Plant Applications," *Proceedings of 21st Symposium on Engineering Aspects of MHD*, Argonne, Ill., June 1983, pp. 1.1.1-1.1.12.

[2]Kessler, R., McClaine, A. W., and Solbes, A., "High Interaction Subsonic MHD Channel Operation," *Journal of Energy*, Vol. 4, May-June 1980, pp. 120-125.

[3]McClaine, A. W., Swallom, D. W., and Kessler, R., "Performance Characteristics of a Subsonic MHD Generator in the Diagonal Mode," *Proceedings of 21st Symposium on Engineering Aspects of MHD*, Argonne, Ill., June 1983, pp. 3.4.1-3.4.10.

[4]McClaine, A. W., Swallom, D. W., and Kessler, R., "Performance Characteristics of Subsonic Generators," *Proceedings of 20th Symposium on Engineering Aspects of MHD*, Irvine, Calif., June 1982, pp. 4.1.1-4.1.5.

[5]McClaine, A. W., Kessler, R., and Swallom, D. W., "Experimental Investigation of Subsonic Combustion Driven MHD Generator Performance," *Proceedings of 19th Symposium on Engineering Aspects of MHD*, Tullahoma, Tenn., June 1981, pp. 1.1.1-1.1.7.

[6]Ikeda, S., Masuda, T., Kusaka, Y., Honda, T., and Aiyama, Y., "Experiment on MHD Generator with a Large-Scale Superconducting Magnet (ETL Mark V)," *AIAA Journal*, Vol. 14, Nov. 1976, pp. 1655-1656.

[7]Ikeda, S., Masuda, T., Kusaka, Y., and Honda, T., "Experiment on MHD Generator with a Large Scale Superconducting Magnet (ETL Mark V)," *Proceedings of 15th Symposium on Engineering Aspects of MHD*, Philadelphia, May 1976, pp. IV.4.1-IV.4.8.

[8]Demetriades, S. T., Maxwell, C. D., and Oliver, D. A., "Progress in Analytical Modelling of MHD Power Generators II," *Proceedings of 21st Symposium on Engineering Aspects of MHD*, Argonne, Ill., June 1983, pp. 3.1.1-3.1.20.

[9]Vanka, S. P. and Ahluwalia, R. K., "Coupled Three Dimensional Flow and Electrical Calculations for Faraday MHD Generators," *Journal of Energy*, Vol. 7, Jan-Feb 1983, p. 65-72.